Forest Ecology and Management 548 (2023) 121404

Contents lists available at ScienceDirect

Forest Ecology and Management

journal homepage: www.elsevier.com/locate/foreco

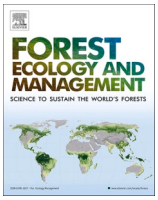

Salinity exposure affects lower-canopy specific leaf area of upland trees in a coastal deciduous forest

Ben Bond-Lamberty [a,*], Lillie M. Haddock [a], Stephanie C. Pennington [a], U. Uzay Sezen [b], Jessica Shue [b], J. Patrick Megonigal [b]

[a] Joint Global Change Research Institute, Pacific Northwest National Laboratory, 5825 University Research Ct. #3500, College Park, MD 20740 USA
[b] Smithsonian Environmental Research Center, 647 Contees Wharf Road, Edgewater, MD 21037, USA

ARTICLE INFO

Keywords:
Forest Ecology
Tree Physiology
Salinity
Leaf area

ABSTRACT

Sea level rise and increasing storm surges are likely to affect the canopy physiology, ecology, and structure of coastal forests, even well in advance of tree mortality. Laboratory and greenhouse studies have documented that saltwater exposure can trigger changes in leaf-level physiology and morphology, but few *in situ* studies have examined how tree-specific leaf area (SLA), the ratio of leaf area to mass and a crucial trait and model parameter, is affected by saline soils. We conducted an observational study of SLA in a mid-Atlantic (USA) coastal deciduous forest, taking advantage of a natural gradient in salinity along a tidal creek. Measured SLA of the 239 trees and seven species sampled ranged from *Carya glabra* (N = 6 trees, mean SLA = 277.9 ± 36.3 cm^2/g) to *Fagus grandifolia* (N = 60, 321.9 ± 62.9 cm^2/g); as expected, trees species and canopy position (sun versus shade) significantly affected SLA. For trees (N = 100) directly exposed to the tidal creek, salinity was highly significant after accounting for species ($P < 0.001$), with trees in the lower reaches of the creek having lower SLA. Leaf area index (LAI), computed from SLA and litter traps, ranged from 4.8 to 15.8 and was inversely related to salinity exposure; the spatial variability in leaf litter production contributed much more to LAI uncertainty than did SLA variability. These *in situ* results are correlative but consistent with the hypothesis, based on previous greenhouse studies, that the stress of chronic salinity exposure changes species' leaf morphology. Our findings are useful for understanding the growing effects of saltwater intrusion into upland forests, as well as parameterizing and testing ecosystem-scale models simulating forest stressors and disturbances at the terrestrial-aquatic interface.

1. Introduction

Rising sea levels and increased storm surges driven by 21st-century climate change are affecting coastal forests in many regions worldwide (McDowell et al., 2022; Kirwan and Gedan, 2019; Williams, 2013), including the heavily forested mid-Atlantic eastern U.S. (Haer et al., 2013; Woods et al., 2020; Fernandes et al., 2018). This combination of press and pulse disturbance can trigger significant and widespread mortality of upland tree species (Ury et al., 2021), but even low levels of increased water and/or salt in the soil may cause poorly understood changes in the canopy physiology, ecology, and structure of these forests (Chen and Kirwan, 2022), changes likely to cascade through energy, water, and nutrient cycles given the dominant role of leaves in terrestrial ecosystems (Fahey et al., 2022).

It has been known for decades that increasing saltwater intrusion into coastal forests results in physiological changes that limit carbon uptake, reduce growth (Wang et al., 2020; Fernandes et al., 2018), and increase tree mortality (Pezeshki et al., 1990; Zhai et al., 2018). Soil salinity also inhibits germination by upland species (Woods et al., 2020), changing the composition of future coastal forests. Many of the effects of saline soil revolve around hydraulic conductance and photosynthesis changes induced by hypoxia and/or salinity (Negrão et al., 2017; McDowell et al., 2022), but salinity exposure is also known to affect leaf morphology in some species (Bray and Reid, 2002; Rodríguez et al., 2005; Cavalcante et al., 2018). Such studies tend to be laboratory- or greenhouse-based; there are few *in situ* observations of how leaf structure and total mass (in particular, total leaf area index or LAI) might be affected by chronic salinity exposure (Vovides et al., 2014).

One crucial leaf structural trait is specific leaf area (SLA), the ratio of one-sided fresh leaf area to leaf dry mass. SLA encapsulates tradeoffs plants make between biomass production, light interception, and nutrient and water conservation (Reich et al., 2007; Greenwood et al.,

* Corresponding author.
E-mail address: bondlamberty@pnnl.gov (B. Bond-Lamberty).

https://doi.org/10.1016/j.foreco.2023.121404
Received 5 June 2023; Received in revised form 1 September 2023; Accepted 2 September 2023
Available online 12 September 2023
0378-1127/© 2023 Battelle Memorial Institute and The Author(s). Published by Elsevier B.V. This is an open access article under the CC BY license (http://creativecommons.org/licenses/by/4.0/).

2017). It is thus a critical parameter for vegetation models and the prediction of plant form and function (Díaz et al., 2022; Park and Jeong, 2021), linked with plant mortality (Greenwood et al., 2017), and needed to compute biometric LAI and associated fluxes (Ewers et al., 2005; Bond-Lamberty et al., 2002). SLA variability is correlated with soil pH (Maire et al., 2015), nutrient availability (Cunningham et al., 1999; Niinemets et al., 1999), and environmental conditions more generally (Wang et al., 2023; Liu et al., 2023). Greenhouse experiments have shown that leaf structure and physiology, to which SLA is tightly tied, are affected by water and salt stresses (Cavalcante et al., 2018; Bray and Reid, 2002; Rodríguez et al., 2005). The uncertainty of how SLA varies with real-world salinity exposure, combined with the sensitivity of most models to SLA parameterization (LeBauer et al., 2013; Chen et al., 2023; Shiklomanov et al., 2020), results in significant predictive uncertainty for ecosystem- to global-scale models making predictions at terrestrial-aquatic interfaces such as coastal forests (Field et al., 2016; Ward et al., 2020).

This observational study of SLA was conducted in coastal deciduous forests at the Smithsonian Environmental Research Center (SERC) in Maryland, USA, taking advantage of a natural gradient in salinity along a tidal creek. We sampled multiple species at both shoreline (hydrologically connected to the creek) and upland plots along this natural gradient. Our goals were to: (i) characterize SLA across a broad range of species, elevations, and canopy heights in these forests; (ii) compare same-species SLA values along the creek's salinity gradient to infer how salinity exposure affects this crucial leaf structural property; and (iii) for a more complete picture of canopy dynamics, estimate biometric leaf area index using SLA and litterfall data (Eriksson et al., 2005) using a Monte Carlo sampling approach to quantify the sources of uncertainty in these estimates. Our primary hypothesis was that SLA would be inversely correlated with chronic exposure to salinity (i.e., shoreline trees at downstream sites along Muddy Creek).

2. Material and methods

This study was conducted in the mid-Atlantic USA at the Smithsonian Environmental Research Center (SERC) in Edgewater, MD, USA, using a series of sites along Muddy Creek (Fig. 1). The region has a mean annual precipitation of 1001 mm and mean annual temperature of 12.9 °C (Pitz and Megonigal, 2017). The upland and shoreline forests sampled here are ~ 60 years old and dominated by the deciduous broadleaf hardwoods *Liriodendron tulipifera*, *Fagus grandifolia*, and *Quercus* spp. (Parker et al., 1989). The parent material is primarily fluvial marine deposits with some areas of overlying alluvium and loess; soil types vary between Collington, Wist, and Annapolis soils (fine-loamy, active, mesic Typic Hapludults) (Correll, 1974; Yang et al., 2020). Shoreline forests occur along Muddy Creek, a third-order stream draining into the Chesapeake Bay, and are hydrologically connected with the creek (Jordan et al., 1991).

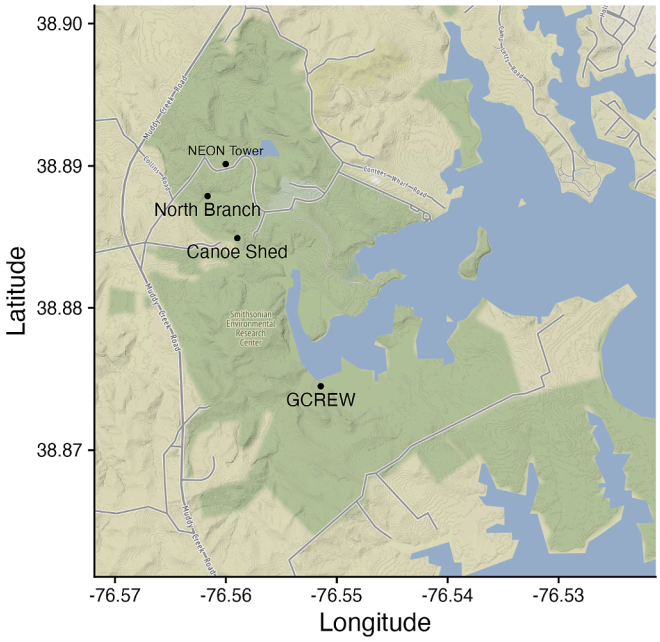

Fig. 1. Map of sites sampled along Muddy Creek, MD, USA, in this study: the low-salinity North Branch site, the medium-salinity Canoe Shed, and the high-salinity Global Change Research Wetland (GCReW). The nearby NEON (Schimel et al., 2007) tower is also shown. The area shown in green is all part of the Smithsonian Environmental Research Center (SERC).

The sample sites were located by the relatively high-salinity creek mouth (38.875 °N, 76.552 °W; "GCReW" in Fig. 1) and roughly one (38.884 °N, 76.557 °W; "Canoe Shed") and two (38.887 °N, 76.562 °W; "North Branch") km upstream. All sites had one plot immediately adjacent to the creek, and two others farther uphill ~ 50 m away from the creek and ~ 5 m higher in elevation. Full tree inventories were conducted in each plot (Pennington et al., 2020). Data from water monitoring wells equipped with conductivity data loggers (HOBO U24-001) were used to estimate the annual salinity average and range experienced at each site. In general the creek experienced oligohaline conditions (0.5–5.0 ppt), decreasing across the three sites from approximately 5.3 ± 3.2 ppt at GCReW to 4.1 ± 2.7 ppt at Canoe Shed to 1.1 ± 0.5 ppt at North Branch (Hopple et al., 2022). However, the midstream and downstream sites also experienced mesohaline conditions (5.0–18.0 ppt) in different seasons (Jordan et al., 1991), with maximum salinities decreasing from 14.9 to 10.1 to 2.9 ppt with increasing distance upstream (Fig. 1).

2.1. Specific leaf area

In summer and early autumn 2019, we sampled a wide variety of trees and tree species across these sites to estimate leaf specific area (SLA). Samples were collected from seven primary species including *Acer rubrum* (Red maple), *Carya glabra* (Pignut hickory), *Fagus grandifolia* (American beech), *Liquidambar styraciflua* (Sweet gum), *Liriodendron tulipifera* (Tulip poplar), *Nyssa sylvatica* (Black gum), and *Quercus alba* (White oak). The samples were collected from two forest positions: shoreline and upland, with 4–6 individual samples of each species per position. We attempted to collect samples from both high-canopy (sun) and low (shade) leaves, but in this tall (20–30 m) forest, sun leaves were frequently inaccessible. Samples from a given tree and tree position (~6 leaves each) were collected using steel pruning shears, a 4.5 m compound bypass pole pruner, or in some cases by shooting them down using a modified crossbow with a fishing line and bolts carrying variable weight tips. Samples were immediately placed in sealed plastic bags and returned to the laboratory within 3–4 h of collection in the field.

In the laboratory, we measured projected fresh leaf area (i.e. the combined area of the leaves in each sample) using a LICOR Leaf Area Meter LI-3100C on the day of collection. The LI-3100C was calibrated to area standards each day. After wiping off any surface water or residue, we measured and recorded the sample leaves' combined area to the nearest 0.01 cm^2. Each group of leaves was then placed in a paper coin envelope and dried in an oven for 72 h at 60 °C. Total dry mass, in grams, was measured to the nearest 0.01 g. Mean SLA was computed for each sample as total fresh area (cm^2) divided by dry mass (g). We did not correct for diurnal changes in leaf water status, assuming that the effect of such variability is small (Garnier et al., 2001). Comparison SLA data were also downloaded (on 2020–07-04, request 10896, open access data only) from the TRY database (Kattge et al., 2020) for the seven species sampled.

2.2. Leaf litterfall and leaf area index

Leaf litter was collected from October 1, 2018 through September 30, 2019. Each plot had six 0.5 m^2 litter traps constructed from PVC pipe and window screen mesh according to the ForestGEO design (https://forestgeo.si.edu/sites/default/files/litterfall_protocol_2010.pdf). Leaf litter was collected approximately once a week in the autumn months, i.e. during maximum leaf fall, and once per month the rest of the year. Leaf litter was dried in an oven for 72 h at 60 °C, sorted into dominant species (*F. grandifolia*, *L. tulipifera*, *Q. alba*, and "other"), and weighed to the nearest 0.1 g. Annual litterfall was then calculated for each species, trap, plot, and site by summing across the entire year of collection. For contextual purposes we also downloaded 2016–2020 litterfall data (dataset NEON.DOM.SITE.DP1.10033.001) from the nearby NEON tower (National Ecological Observatory Network, 2021).

Leaf area index—the one-sided green leaf area per unit ground area—was calculated (Fang et al., 2019) for each plot by multiplying litterfall (g m^{-2}) by SLA (cm^2 g^{-1}), after converting the latter to m^2 g^{-1}. We did this on a species-specific basis for *F. grandifolia*, *L. tulipifera*, and *Q. alba*, the three trees for which litter was sorted to a specific-specific level. For the remaining leaf litter, we calculated an "other" SLA value as the mean of *A. rubrum*, *C. glabra*, *L. styraciflua*, and *N. sylvatica*, weighting by the sum of the square of tree diameters for each species—i.e., by biomass and thus approximate expected leaf area—using the tree inventory data from each plot (Pennington et al., 2020). Leaf area values were then summed by species to the litter trap level, with the plot mean and standard deviation computed across all traps.

2.3. Statistical analysis

Differences in SLA across species and canopy position (sun versus shade) were tested by constructing an Analysis of Variance Model (Venables and Ripley, 2003) with these two terms and their interaction; Tukey Honest Significant Differences (HSD) were then computed using the *HSD.test* function from R's *agricolae* package version 1.3–1 (de Mendiburu, 2019). A paired Student's *t*-test was also used to test for sun versus shade leaf differences in SLA, using data from the subset of trees for which we took samples from both canopy positions. Elevation effects (i.e. SLA differences between low-elevation trees by Muddy Creek and those up-slope) were tested similarly, using an ANOVA with species and elevation as interacting terms and then an HSD test. The effect of changing salinity (i.e., site differences along the Muddy Creek salinity gradient) were also tested using this approach, but using only the subset of trees at low elevations and thus directly exposed to creek waters. Species-specific distributional differences between SLA computed in this study and data from TRY were quantified using R's Kolmogorov-Smirnov test (*ks.test*).

To quantify the sources of uncertainty in our computation of leaf area index, we used a Monte Carlo resampling approach. We first performed 1000 random draws of the SLA estimates, using the plot- and species-specific means and standard deviations to generate new, normally-distributed SLA values that were then multiplied by constant litterfall data to produce leaf area as described above. A second resampling generated 1000 random instances of litterfall, using the trap-to-trap mean and standard deviations from each plot to construct Normal distributions that were multiplied by constant SLA means. A third resampling combined both sources of uncertainty (i.e., using random realizations of both SLA and litterfall). Overall median and 95% confidence intervals were then computed from the resulting *post hoc* distributions.

2.4. Data and code availability

Analyses were performed using the R language for statistical computing version 4.1.3 (R Core Team, 2021). Maps were made using R's *ggmap* package (Kahle and Wickham, 2013).

All code and data used in this analysis are available at https://github.com/COMPASS-DOE/SLA, and permanently archived at https://dx.doi.org/10.5281/zenodo.8319160. The data are deposited at ESS-DIVE as well (https://dx.doi.org/10.15485/1998945). In addition, roughly two-thirds of the SLA data (from measurements in June and July 2019) were incorporated into the most recent release of the TRY database (Kattge et al., 2020) and thus available at https://www.try-db.org/.

3. Results

3.1. Specific leaf area

In total, we measured SLA for a total of 239 samples, with each consisting of on average six leaves (with a minimum of 3 and a maximum of 13). The seven tree species sampled ranged from *C. glabra* (N = 6, mean SLA = 277.9 cm^2 g^{-1}) to *F. grandifolia* (N = 60, SLA = 321.9 cm^2 g^{-1}) (Table 1). Accessing the upper canopy of this tall deciduous forest was difficult: we obtained 201 samples from low height, i.e. from shade leaves, but only 38 from high sun leaves. Across all our SLA samples, 100 were from shoreline trees directly exposed to the salinity gradient of Muddy Creek, while 139 came from up-slope trees.

In a linear model with species and canopy position as interacting terms predicting SLA, both terms were highly significant: species ($F_{1,6}$ = 21.167, $P < 0.001$) and position ($F_{1,1}$ = 14.265, $P < 0.001$); their interaction was not ($F_{1,5}$ = 1.425, P = 0.216). A Tukey's HSD test categorized the SLA values in this model into five groups, summarized visually in Fig. 3. Because high- and low-canopy samples were frequently taken from common trees, we also used a paired T-test to examine the effect of canopy position. This was also significant (T_{35} = -8.419, $P < 0.001$), indicating, as expected, that high-position (sun) leaves tended to have significantly lower SLA than low (shade) leaves.

Two species exhibited strong negative relationships between tree diameter (cm) and leaf SLA (cm^2 g^{-1}): *L. styraciflua* (SLA = -2.991D + 275.1, P = 0.001) and *N. sylvatica* (SLA = -4.112D + 321.5, $P < 0.001$). Two others were marginally significant: *A. rubrum* (SLA = -1.071D + 214.5, P = 0.084) and *L. tulipifera* (SLA = -2.989D + 361.6, P = 0.051). Tree diameter was unrelated to SLA for the other three species (Fig. 2).

As noted above, roughly 40% of our trees were shoreline, while the others were up-slope, away from Muddy Creek. This elevation effect was marginally significant after accounting for species ($F_{1,1}$ = 3.511, P = 0.062), and the interaction between species and elevation was significant ($F_{1,4}$ = 2.871, P = 0.024). Of the five species that occurred at both low and higher elevations, this effect on SLA was highly significant for *Q. alba* (P = 0.001), significant ($0.01 < P < 0.05$) for *N. sylvatica* and *A. rubrum*, marginally significant (P = 0.076) for *F. grandifolia*, and not significant for *L. styraciflua* (P = 0.653).

Our central hypothesis was that salinity exposure would negatively affect tree SLA. In an overall analysis of variance on the subset of trees occurring directly by the creek (N = 100), this salinity effect was highly significant after accounting for species ($F_{1,2}$ = 12.439, $P < 0.001$), but the interaction between species and salinity was not ($F_{1,6}$ = 0.703, P = 0.648). In general, there was no difference in SLA between the two

Table 1
Specific leaf area (SLA, cm^2/g) for the seven tree species samples at three different sites along Muddy Creek, MD, USA. Number of samples (N, each consisting of ~ 6 separate leaves) and standard deviation of sample SLA are also given.

Species	N	SLA	s.d.
Acer rubrum	39	193.7	39.0
Carya glabra	6	277.9	36.3
Fagus grandifolia	60	321.9	62.9
Liquidambar styraciflua	42	224.5	93.4
Liriodendron tulipifera	20	237.8	96.9
Nyssa sylvatica	37	261.2	86.1
Quercus alba	35	192.0	37.4

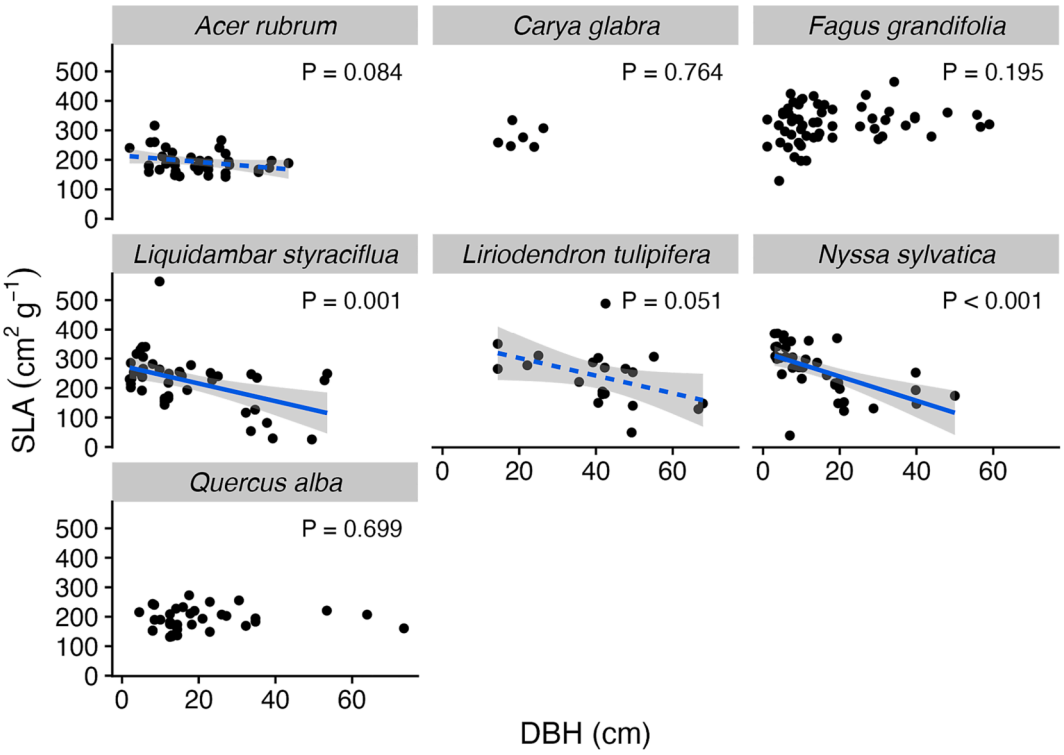

Fig. 2. Tree diameter at breast height (DBH, as measured at ~ 1.4 m) versus specific leaf area (SLA), by species. Each point represents a sample consisting of ~ 6 separate leaves. Regression lines and accompanying p-values are shown; solid lines are significant at a level of α = 0.05, and dashed lines at α = 0.10.

lower-salinity upstream sites, and thus we proceeded with species-specific tests that compared the high-salinity GCREW site (cf. Fig. 1) versus the other two. SLA was numerically smaller under high-salinity conditions for all five species tested (Table 2), and this difference was statistically significant for three: *A. rubrum* (P = 0.021), *L. styraciflua* (P = 0.002), and *N. sylvatica* (P = 0.035).

We used 1790 species-specific observations from the TRY database (Kattge et al., 2020) to put our SLA observations into a broader context (Fig. 4). In general the SLA distributions in this study were significantly different (P < 0.001) from the distributions in TRY. The two exceptions were *L. tulipifera* (D = 0.350, P = 0.203) and *N. sylvatica* (D = 0.364, P = 0.068).

3.2. Litterfall and leaf area index

Litter production peaked during the autumn in these temperate forest sites (Fig. 5). Mean annual production was 374.7 g m^{-2}, with an average spatial variability (i.e. between litter traps within a plot) of 39.3 g m^{-2}. These values were consistent with data from the nearby NEON tower (Fig. 5). Across all plots, *F. grandifolia* dominated, comprising 31% of total mass.

Overall leaf area index (LAI, m^2 m^{-2}) inferred from the combination of SLA and litterfall data ranged from 4.8 with a 95% confidence interval of (3.0, 6.6) in the high-elevation, medium-salinity "Canoe Shed" plot, to a very high value of 15.8 (9.8, 21.7) in the mid-elevation plot at the low-salinity "North Branch" site. The low-elevation plots' LAI values were inversely related to their salinity exposure, with values from 8.9 (6.0, 11.8) at the high-salinity site, to 9.7 (7.0, 12.5), to 11.5 (5.9, 17.1) at the lowest-salinity site. Spatial variability in leaf litter production contributed much more to the uncertainty in LAI estimates than did variability in the SLA measurements (**Supplementary Figure 1**).

Table 2
Specific leaf area (SLA, cm^2/g) across the tidal salinity gradient of Muddy Creek, by species, at the three sites sampled. The "Low" salinity site is North Branch; "Medium" is Canoe Shed; and "High" is GCReW on the map (Fig. 1). Values are mean ± s.d., with the number of samples given in parentheses. Two species from Table 1, *Carya glabra* and *Liriodendron tulipifera*, did not occur at shoreline positions and thus do not appear here. High-salinity SLA values that are significantly lower than the low and medium values are marked with * (P < 0.05) or ** (P < 0.01).

Species	Low	Medium	High
Acer rubrum		213.3 ± 50.9 (4)	171.6 ± 21.7 (15) *
Fagus grandifolia	344.5 ± 45.2 (6)	371.6 ± 51.6 (6)	312.8 ± 60 (5)
Liquidambar styraciflua	263.2 ± 42.3 (6)	247.5 ± 10.9 (2)	189.8 ± 44.8 (12) **
Nyssa sylvatica	253.9 ± 118.6 (6)	275.8 ± 53.9 (6)	192 ± 42.2 (9) *
Quercus alba	193.2 ± 27.5 (6)		172.5 ± 35.7 (17)

4. Discussion

Specific leaf area is a key and widely-studied trait in the leaf economics spectrum (Wright et al., 2004), and many of our results are consistent with previous SLA studies and syntheses. We found strong effects of species and canopy height on SLA (Fig. 3), consistent with the general pattern that SLA tends to increase lower in the canopy (e.g. Xiao et al., 2006; Sellin and Kupper, 2006; Marshall and Monserud, 2003), where leaves are optimized for light-gathering as opposed to protecting photosynthetic machinery and minimizing stomatal water loss (Kozlowski and Pallardy, 1997). We also found that lower-slope (i.e., creek-adjacent) trees tended to have lower SLA than their upper-slope counterparts after controlling for species. This is in contrast to patterns over larger spatial scales where climatic rather than soil variables tend to be stronger predictors of SLA variability (Maire et al., 2015). Four of the seven species measured here also exhibited a negative correlation between tree diameter and SLA (Fig. 2), an effect that has been found to be associated with smaller, higher-SLA trees having higher photosynthetic capacity (Liu et al., 2010).

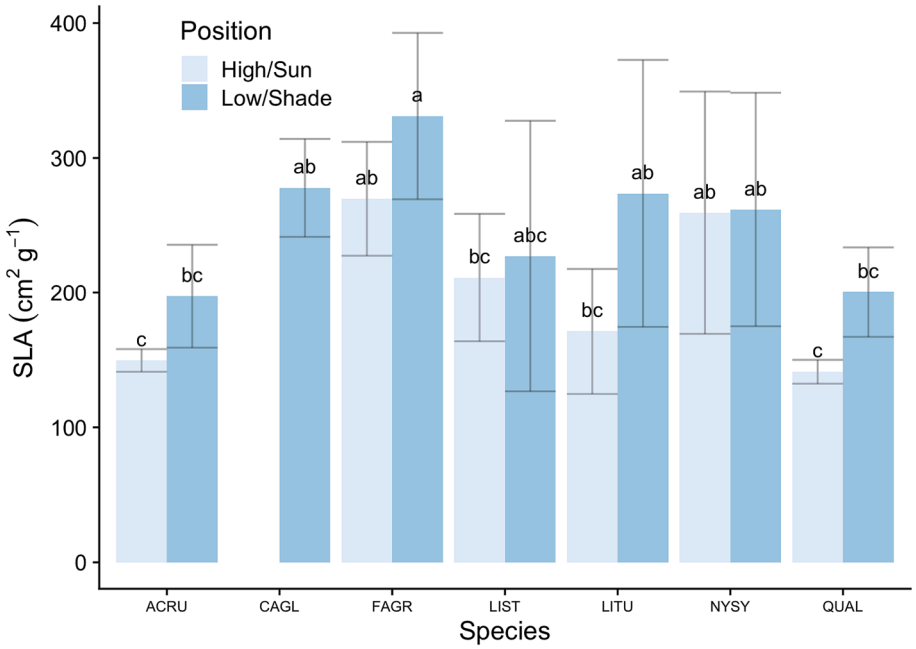

Fig. 3. Mean specific leaf area (SLA) by species and canopy position. Error bars indicate standard deviation between samples; letter groupings are based on Tukey's HSD test. Species codes: *Acer rubrum* (ACRU), *Carya glauca* (CAGL), *Fagus grandifolia* (FAGR), *Liriodendron tulipifera* (LITU), *Liquidambar styraciflua* (LIST), *Nyssa sylvatica* (NYSY), and *Quercus alba* (QUAL).

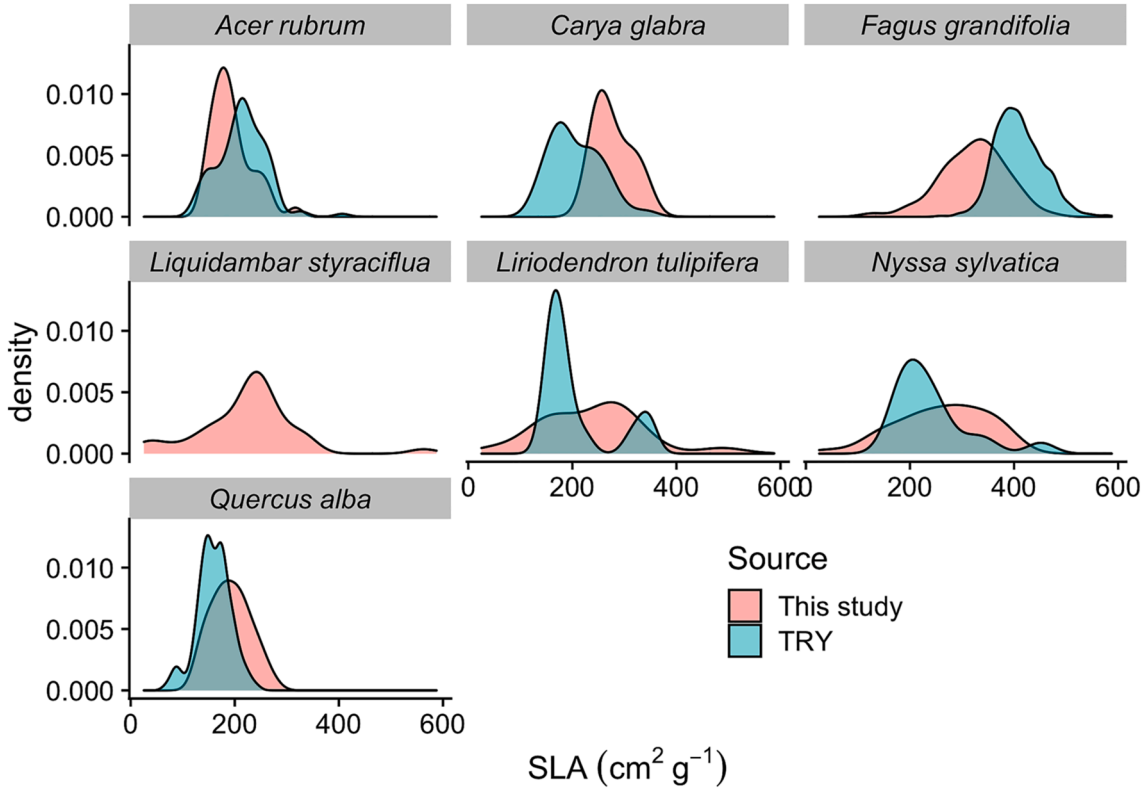

Fig. 4. Distribution of specific leaf area (SLA) samples from this study versus those in the TRY database (Kattge et al., 2020), by species.

The ranges of our measured SLA values were broadly consistent with a previous study in this same watershed (Parker et al., 1989), as well as observations in the TRY database (Fig. 4). However, the distributions were generally different, which may be an unavoidable artifact of the relatively small (relative to TRY) number of samples in this study. SLA is one of the most-frequently measured plant traits, with tens of thousands of observations in TRY (Kattge et al., 2020), but the parameter is central to plant resource tradeoffs (Díaz et al., 2022) and so influential in most ecophysiological process models that it remains worth measuring when possible (Shiklomanov et al., 2020).

We found that exposure to increased salinity was associated with reduced SLA: shoreline trees growing in the lower, more-saline reaches

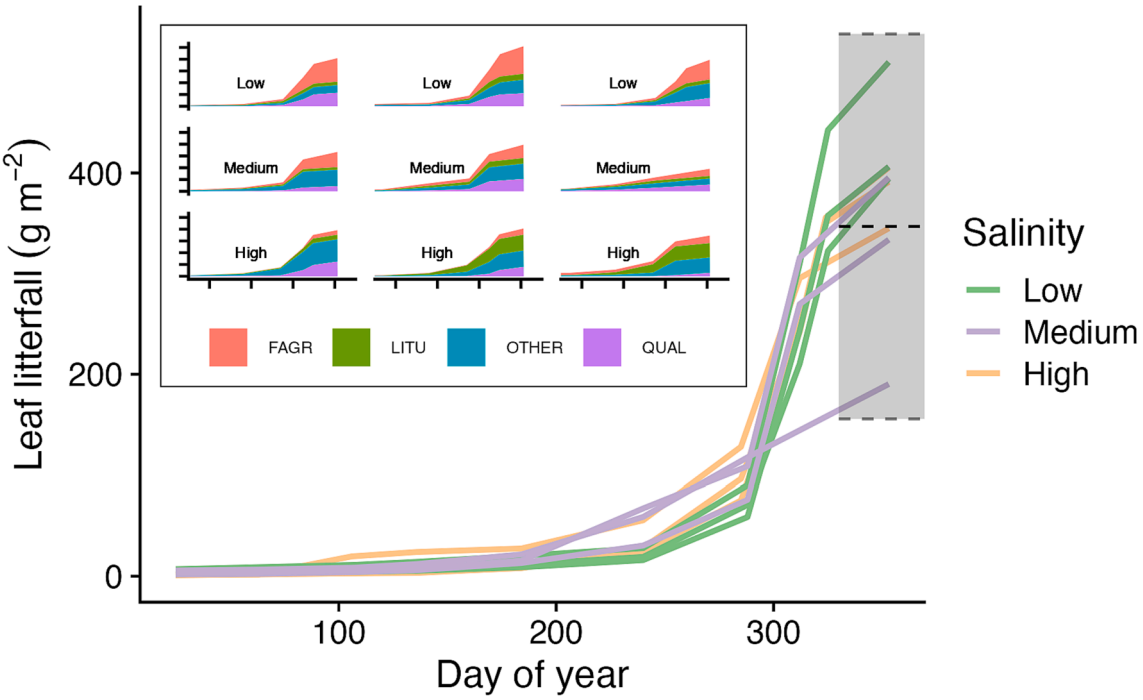

Fig. 5. Cumulative leaf litterfall, based on N = 6 litter traps (each 0.5 m^2), by day of year and colored by creek salinity (cf. Fig. 1). Each line represents a different sample plot; the grey region shows the range (median, dark dashed line, with ± 1 standard deviation as lighter dashed lines) of annual litterfall measured at the nearby NEON tower. Inset plot shows data for each of the nine plots, labeled by creek salinity level (Low/Medium/High) and species (*Fagus grandifolia*, FAGR; *Liriodendron tulipifera*, LITU; *Quercus alba*, QUAL; and other); for visual clarity, these are shown only for the second half of the year.

of the tidal creek studied here had lower-SLA leaves (Table 2), and this difference was statistically significant for *A. rubrum*, *L. styraciflua*, and *N. sylvatica*. Salt exposure is stressful for plants (Munns, 2002), negatively affecting growth and eventually increasing mortality due to the osmotic and toxic effects of high ion concentrations in soils (McDowell et al., 2022; Negrão et al., 2017). Such external stresses can cause plants to change their physiological and/or morphological characteristics. In a greenhouse study of the aquatic fern *Salvinia natans*, plants grown under high salinities produced smaller and thicker leaves, likely because osmotic stress and lowered turgor pressure restricted cell expansion (Jampeetong and Brix, 2009). Similar effects have been observed in agricultural studies, for example salinity-induced morphological changes in *Phaseolus vulgaris* (Bray and Reid, 2002). Conversely, a greenhouse experiment using *Jatropha curcas*, a plant relatively tolerant of saline conditions, found physiological changes but no shifts in biomass allocation under high salinity levels (Cavalcante et al., 2018).

In situ observational studies have also reported plant trait and morphological changes along salinity gradients consistent with our results. Many mangroves exhibit morphological plasticity due to the effects of salinity (Mollick et al., 2021; Cao et al., 2023), and at the population level SLA is highest in freshwater zones (Azad et al., 2022). Even small salinity gradients can be associated with structural and functional changes. In a forested wetland in South Carolina, USA, trees exhibited physiological changes that reduced water use, growth, and biomass at a low (~3 psu) salinity level (Duberstein et al., 2020), a similar range to the Muddy Creek system studied here. Although there is ample reason to think that the SLA of upland trees would be reduced by chronic, non-lethal exposure to salinity, we are unaware of any previous study quantifying the magnitude of this effect. An important caveat here is that we were able to obtain only a few samples from top-of-canopy sun leaves, and thus our inferred salinity effects apply only to the lower canopy; future studies should prioritize a fuller sampling across the full vertical canopy profile (e.g. Sellin and Kupper 2006).

Our estimates of plot-level total leaf area index (LAI) varied threefold. The lower end of these estimates overlapped with values of 5.26 and 7.1 reported in previous studies within the same watershed (Parker et al., 1989; Parker and Tibbs, 2004). The upper end value (15.8) occurred at the upstream North Branch site (Fig. 1), at the southwest corner of the SERC ForestGEO plot (Anderson-Teixeira et al., 2015). This mid-slope plot had a well-developed *F. grandifolia* understory producing 234 g m^{-2} of leaf litter annually, several large (>100 cm DBH) oak trees producing 111 g m^{-2}, and a significant *L. tulipifera* presence. Including other species, the plot litter total was thus 510 g m^{-2} yr^{-1}, at the upper range of values recorded by the nearby NEON tower (Fig. 5), and had an overall weighted mean SLA of 310 cm^2 g^{-1}, again well within observed ranges (Fig. 4). We conclude that this 15.8 LAI value is unusually large but also realistic, and at the upper end of other litter-based estimates in deciduous forests (Bolstad et al., 2001; Le Dantec et al., 2000; Ishihara and Hiura, 2011). This testifies to the large range of LAI across forested landscapes, but also to the importance of direct, laborious measurements to obtain "true LAI" (Fang et al., 2019) values against which optical and other indirect measurement techniques can be checked.

Leaf area declined in the downstream, more-saline lower watershed, driven by lower mean SLA (Table 2), consistent with previous work documenting structural spatial variability driven by salinity exposure (Duberstein et al., 2020). However, within individual plots we used a novel Monte Carlo analysis to show that the variability in LAI estimates was driven by spatial variability in litterfall, not uncertainty in the SLA estimates (**Supplementary Figure 1**). This is consistent with Ishihara and Hura (2011), who found that LAI of a deciduous temperate forest could be modeled most accurately by accounting for the spatial heterogeneity of leaf litterfall. Optical LAI methods can potentially underestimate the resulting LAI variability in temperate deciduous forests (Le Dantec et al., 2000; Zheng and Moskal, 2012; Mussche et al., 2001).

Several weaknesses of this study should be noted. First and importantly, observational studies such as this one can infer causality but not prove it (Larsen et al., 2019). Here, the salinity gradient in Muddy Creek (Fig. 1) is real—see the Methods—as is its correlation with SLA and LAI for shoreline plots directly exposed to the creek's hydrology, but it is possible that one or more other confounding factors are the real driver of

these leaf-level changes. Nonetheless, as noted above, the direction of SLA change along the creek is consistent with previous greenhouse studies in which salinity was directly manipulated, and we believe that *in situ* but observational studies taking advantage of such natural gradients are valuable as long as they are complemented by manipulative and modeling work (Davies and Gray 2015). Second, as noted above, we could obtain only a few leaf samples from the high canopy, limiting our ability to probe the interaction between leaf sun/shade status and salinity exposure. The advent of unmanned aerial vehicles able to cut and retrieve leaf samples promises to open new frontiers for quantifying the structure and function of such high-canopy leaves (Anderson and Gaston, 2013; Käslin et al., 2018).

There are a number of broader implications if tree SLA is affected by chronic salinity exposure *in situ*. First, these results can support a better understanding of the processes that stress and ultimately kill coastal trees (Kirwan and Gedan, 2019; Ury et al., 2021)(McDowell et al., 2022; Kirwan and Gedan, 2019; Ury et al., 2021). Our work could thus potentially provide an early warning metric as SLA values in increasingly stressed coastal forests transition from 'upland' to 'low salinity exposed' to 'high salinity exposed' ranges. Our findings can also help with model uncertainty quantification; SLA is useful to upscale gross primary production, vegetation community composition, and other parameters in Earth System Models (Bonan et al., 2012), and site-specific SLA observations can improve predictions of future vegetation structure and function in terrestrial ecosystems, while providing important present-day constraints against which such models can be benchmarked (Sinha et al., 2023; Walker et al., 2014). This is crucial, because greenhouse and laboratory experiments, while valuable, will not be sufficient to understand and predict the integrated effects of climate change, rising sea levels, and increasing storms in coastal forests (Duberstein et al., 2020). Rather, a combination of observational and large-scale ecosystem manipulations (Hopple et al., 2023) will be needed for robust understanding and prediction of these rapidly-changing ecosystems at the terrestrial-aquatic interface.

5. Conclusions

This study took advantage of a natural salinity gradient of a temperate forest creek to study how differences in species, canopy position, and salinity exposure were associated with changes in SLA. Trees directly exposed to the tidal creek had lower SLA in higher-salinity plots; these plots also had lower total leaf area index. Our *in situ*, observational study cannot exclude all potential confounding factors; nonetheless, its results are consistent with greenhouse studies reporting that the stress of chronic salinity changes the leaf morphology and physiology of trees. We conclude that incipient ecosystem state shifts at the coastal interface may be predictable by observing changes in leaf-level parameters such as SLA, changes that typically precede tree death and the formation of ghost forests (McDowell et al. 2022). Further integrated research using both models and larger-scale manipulative field experiments are crucial to fully understanding the structural and functional changes in coastal forests worldwide.

CRediT authorship contribution statement

Ben Bond-Lamberty: Conceptualization, Funding acquisition, Formal analysis, Supervision, Writing – original draft, Writing – review & editing. **Lillie M. Haddock:** Investigation, Formal analysis, Writing – review & editing. **Stephanie C. Pennington:** Investigation, Writing – review & editing. **U. Uzay Sezen:** Investigation, Writing – review & editing. **Jessica Shue:** Investigation, Writing – review & editing. **J. Patrick Megonigal:** Supervision, Writing – review & editing.

Declaration of Competing Interest

The authors declare that they have no known competing financial interests or personal relationships that could have appeared to influence the work reported in this paper.

Data availability

All data and code are openly available and linked in the manuscript.

Acknowledgments

Fieldwork for this study was performed as part of the PREMIS Initiative, a Laboratory Directed Research and Development Program at Pacific Northwest National Laboratory (PNNL), and supported by the Smithsonian Environmental Research Center. L.M.H. was supported by a DOE Science Undergraduate Laboratory Internship (https://science.osti.gov/wdts/suli). Data analysis and writing were supported by COMPASS-FME, a multi-institutional project funded by the U.S. Department of Energy, Office of Science, Biological and Environmental Research, as part of the Environmental System Science Program. PNNL is operated by Battelle for the U.S. Department of Energy (DOE) under Contract DE-AC05-76RL01830.

Appendix A. Supplementary data

Supplementary data to this article can be found online at https://doi.org/10.1016/j.foreco.2023.121404.

References

Anderson, K., Gaston, K.J., 2013. Lightweight unmanned aerial vehicles will revolutionize spatial ecology. Front. Ecol. Environ. 11 (3), 138–146.

Anderson-Teixeira, K.J., Davies, S.J., Bennett, A.C., Gonzalez-Akre, E.B., Muller-Landau, H.C., Joseph Wright, S., Abu Salim, K., Almeyda Zambrano, A.M., Alonso, A., Baltzer, J.L., Basset, Y., Bourg, N.A., Broadbent, E.N., Brockelman, W.Y., Bunyavejchewin, S., Burslem, D.F.R.P., Butt, N., Cao, M., Cardenas, D., Chuyong, G. B., Clay, K., Cordell, S., Dattaraja, H.S., Deng, X., Detto, M., Du, X., Duque, A., Erikson, D.L., Ewango, C.E.N., Fischer, G.A., Fletcher, C., Foster, R.B., Giardina, C.P., Gilbert, G.S., Gunatilleke, N., Gunatilleke, S., Hao, Z., Hargrove, W.W., Hart, T.B., Hau, B.C.H., He, F., Hoffman, F.M., Howe, R.W., Hubbell, S.P., Inman-Narahari, F. M., Jansen, P.A., Jiang, M., Johnson, D.J., Kanzaki, M., Kassim, A.R., Kenfack, D., Kibet, S., Kinnaird, M.F., Korte, L., Kral, K., Kumar, J., Larson, A.J., Li, Y., Li, X., Liu, S., Lum, S.K.Y., Lutz, J.A., Ma, K., Maddalena, D.M., Makana, J.-R., Malhi, Y., Marthews, T., Mat Serudin, R., McMahon, S.M., McShea, W.J., Memiaghe, H.R., Mi, X., Mizuno, T., Morecroft, M., Myers, J.A., Novotny, V., de Oliveira, A.A., Ong, P. S., Orwig, D.A., Ostertag, R., den Ouden, J., Parker, G.G., Phillips, R.P., Sack, L., Sainge, M.N., Sang, W., Sri-ngernyuang, K., Sukumar, R., Sun, I.-F., Sungpalee, W., Suresh, H.S., Tan, S., Thomas, S.C., Thomas, D.W., Thompson, J., Turner, B.L., Uriarte, M., Valencia, R., Vallejo, M.I., Vicentini, A., Vrška, T., Wang, X., Wang, X., Weiblen, G., Wolf, A., Xu, H., Yap, S., Zimmerman, J., 2015. CTFS-ForestGEO: a worldwide network monitoring forests in an era of global change. Glob. Chang. Biol. 21 (2), 528–549.

Azad, S., Mollick, A.S., Setu, F.A., Islam Khan, N., Kamruzzaman,, 2022. Stand structure, tree species diversity, and leaf morphological plasticity in Xylocarpus mekongensis Pierre among salinity zones in the Sundarbans, Bangladesh. J. Asia-Pacific Biodiversity 15, 414–424.

Bolstad, P.V., Vose, J.M., McNulty, S.G., 2001. Forest productivity, leaf area, and terrain in southern appalachian deciduous forests. For. Sci. 47, 419–427.

Bonan, G.B., Oleson, K.W., Fisher, R.A., Lasslop, G., Reichstein, M., 2012. Reconciling leaf physiological traits and canopy flux data: Use of the TRY and FLUXNET databases in the Community Land Model version 4. Journal of Geophysical Research-Biogeosciences 117 (G2), n/a–n/a.

Bond-Lamberty, B., Wang, C., Gower, S.T., Norman, J., 2002. Leaf area dynamics of a boreal black spruce fire chronosequence. Tree Physiol. 22 (14), 993–1001.

Bray, S., Reid, D.M., 2002. The effect of salinity and CO2 enrichment on the growth and anatomy of the second trifoliate leaf of Phaseolus vulgaris. Can. J. Bot. 80 (4), 349–359.

Cao, J.-J., Chen, J., Yang, Q.-P., Xiong, Y.-M., Ren, W.-Z., Kong, D.-L., 2023. Leaf hydraulics coordinated with leaf economics and leaf size in mangrove species along a salinity gradient. Plant Diversity 45 (3), 309–314.

Cavalcante, P.G.d.S., Santos, C.M.D., Filho, H.C.d.L.W., Avelino, J.R.L., Endres, L., 2018. Morpho-physiological adaptation of Jatropha curcas L. to salinity stress. Aust. J. Crop Sci. 12 (04), 563–571.

Chen, Y., Kirwan, M.L., 2022. Climate-driven decoupling of wetland and upland biomass trends on the mid-Atlantic coast. Nat. Geosci. 15 (11), 913–918.

Chen, A., Ricciuto, D., Mao, J., Wang, J., Lu, D., Meng, F., 2023. Improving E3SM land model photosynthesis parameterization via satellite SIF, machine learning, and surrogate modeling. J. Adv. Model. Earth Syst. 15 https://doi.org/10.1029/2022ms003135.

Correll, D.L., 1974. Soil sampling and nutrient analyses in forest ecology sites, Environmental Monitoring and Baseline Data. Compiled Under the Smithsonian Institution Environmental Sciences Program. Temperate Studies 3, 1099–1112.
Cunningham, S.A., Summerhayes, B., Westoby, M., 1999. Evolutionary divergences in leaf structure and chemistry, comparing rainfall and soil nutrient gradients. Ecol. Monogr. 69 (4), 569–588.
Davies, G.M., Gray, A., 2015. Don't let spurious accusations of pseudoreplication limit our ability to learn from natural experiments (and other messy kinds of ecological monitoring). Ecol. Evol. 5 (22), 5295–5304.
de Mendiburu, F.: agricolae: Statistical Procedures for Agricultural Research, 2019.
Díaz, S., Kattge, J., Cornelissen, J.H.C., Wright, I.J., Lavorel, S., Dray, S., Reu, B., Kleyer, M., Wirth, C., Prentice, I.C., Garnier, E., Bönisch, G., Westoby, M., Poorter, H., Reich, P.B., Moles, A.T., Dickie, J., Zanne, A.E., Chave, J., Wright, S.J., Sheremetiev, S.N., Jactel, H., Baraloto, C., Cerabolini, B.E.L., Pierce, S., Shipley, B., Casanoves, F., Joswig, J.S., Günther, A., Falczuk, V., Rüger, N., Mahecha, M.D., Gorné, L.D., Amiaud, B., Atkin, O.K., Bahn, M., Baldocchi, D., Beckmann, M., Blonder, B., Bond, W., Bond-Lamberty, B., Brown, K., Burrascano, S., Byun, C., Campetella, G., Cavender-Bares, J., Chapin, F.S., Choat, B., Coomes, D.A., Cornwell, W.K., Craine, J., Craven, D., Dainese, M., de Araujo, A.C., de Vries, F.T., Domingues, T.F., Enquist, B.J., Fagúndez, J., Fang, J., Fernández-Méndez, F., Fernandez-Piedade, M.T., Ford, H., Forey, E., Freschet, G.T., Gachet, S., Gallagher, R., Green, W., Guerin, G.R., Gutiérrez, A.G., Harrison, S.P., Hattingh, W. N., He, T., Hickler, T., Higgins, S.I., Higuchi, P., Ilic, J., Jackson, R.B., Jalili, A., Jansen, S., Koike, F., König, C., Kraft, N., Kramer, K., Kreft, H., Kühn, I., Kurokawa, H., Lamb, E.G., Laughlin, D.C., Leishman, M., Lewis, S., Louault, F., Malhado, A.C.M., Manning, P., Meir, P., Mencuccini, M., Messier, J., Miller, R., Minden, V., Molofsky, J., Montgomery, R., Montserrat-Martí, G., Moretti, M., Müller, S., Niinemets, Ü., Ogaya, R., Öllerer, K., Onipchenko, V., Onoda, Y., Ozinga, W.A., Pausas, J.G., Peco, B., Penuelas, J., Pillar, V.D., Pladevall, C., Römermann, C., Sack, L., Salinas, N., Sandel, B., Sardans, J., Schamp, B., Scherer-Lorenzen, M., Schulze, E.-D., Schweingruber, F., Shiodera, S., Sosinski, Ë., Soudzilovskaia, N., Spasojevic, M.J., Swaine, E., Swenson, N., Tautenhahn, S., Thompson, K., Totte, A., Urrutia-Jalabert, R., Valladares, F., van Bodegom, P., Vasseur, F., Verheyen, K., Vile, D., Violle, C., von Holle, B., Weigelt, P., Weiher, E., Wiemann, M.C., Williams, M., Wright, J., Zotz, G., 2022. The global spectrum of plant form and function: enhanced species-level trait dataset. Sci. Data 9 (1).
Duberstein, J.A., Krauss, K.W., Baldwin, M.J., Allen, S.T., Conner, W.H., Salter, J.S., Miloshis, M., 2020. Small gradients in salinity have large effects on stand water use in freshwater wetland forests. For. Ecol. Manage. 473, 118308.
Eriksson, H., Eklundh, L., Hall, K., Lindroth, A., 2005. Estimating LAI in deciduous forest stands. Agric. For. Meteorol. 129 (1-2), 27–37.
Ewers, B.E., Gower, S.T., Bond-Lamberty, B., Wang, C., 2005. Effects of stand age and tree species composition on transpiration and canopy conductance of boreal forest stands. Plant Cell Environ. 28, 660–678.
Fahey, T.J., Cleavitt, N.L., Battles, J.J., 2022. Long term variation of leaf abundance in a northern hardwood forest. Ecol. Ind. 137, 108746.
Fang, H., Baret, F., Plummer, S., Schaepman-Strub, G., 2019. An overview of global leaf area index (LAI): Methods, products, validation, and applications. Rev. Geophys. 57 (3), 739–799.
Fernandes, A., Rollinson, C.R., Kearney, W.S., Dietze, M.C., Fagherazzi, S., 2018. Declining radial growth response of coastal forests to hurricanes and nor'easters. J. Geophys. Res. Biogeosci. 123 (3), 832–849.
Field, C.R., Gjerdrum, C., Elphick, C.S., 2016. Forest resistance to sea-level rise prevents landward migration of tidal marsh. Biol. Conserv. 201, 363–369.
Garnier, E., Shipley, B., Roumet, C., Laurent, G., 2001. A standardized protocol for the determination of specific leaf area and leaf dry matter content. Funct. Ecol. 15, 688–695.
Greenwood, S., Ruiz-Benito, P., Martínez-Vilalta, J., Lloret, F., Kitzberger, T., Allen, C.D., Fensham, R., Laughlin, D.C., Kattge, J., Bönisch, G., Kraft, N.J.B., Jump, A.S., Chave, J., 2017. Tree mortality across biomes is promoted by drought intensity, lower wood density and higher specific leaf area. Ecol. Lett. 20 (4), 539–553.
Haer, T., Kalnay, E., Kearney, M., Moll, H., 2013. Relative sea-level rise and the conterminous United States: Consequences of potential land inundation in terms of population at risk and GDP loss. Glob. Environ. Change 23 (6), 1627–1636.
Hopple, A.M., Pennington, S.C., Megonigal, J.P., Bailey, V., Bond-Lamberty, B., 2022. Disturbance legacies regulate coastal forest soil stability to changing salinity and inundation: a soil transplant experiment. Soil Biol. Biochem. 169, 108675.
Hopple, A.M., Doro, K.O., Bailey, V.L., Bond-Lamberty, B., McDowell, N., Morris, K.A., Myers-Pigg, A., Pennington, S.C., Regier, P., Rich, R., Sengupta, A., Smith, R., Stegen, J., Ward, N.D., Woodard, S.C., Megonigal, J.P., 2023. Attaining freshwater and estuarine-water soil saturation in an ecosystem-scale coastal flooding experiment. Environ. Monit. Assess. 195, 425.
Ishihara, M.I., Hiura, T., 2011. Modeling leaf area index from litter collection and tree data in a deciduous broadleaf forest. Agric. For. Meteorol. 151 (7), 1016–1022.
Jampeetong, A., Brix, H., 2009. Effects of NaCl salinity on growth, morphology, photosynthesis and proline accumulation of Salvinia natans. Aquat. Bot. 91 (3), 181–186.
Jordan, T.E., Correll, D.L., Miklas, J., Weller, D.E., 1991. Nutrients and chlorophyll at the interface of a watershed and an estuary. Limnol. Oceanogr. 36 (2), 251–267.
Kahle, D. and Wickham, H.: ggmap: Spatial Visualization with ggplot2, https://journal.r-project.org/archive/2013-1/kahle-wickham.pdf, 2013.
Käslin, F., Baur, T., Meier, P., Koller, P., Buchmann, N., D'Odorico, P., Eugster, W., 2018. Novel twig sampling method by unmanned aerial vehicle (UAV). Frontiers in Forests and Global Change 1. https://doi.org/10.3389/ffgc.2018.00002.
Kattge, J., Bönisch, G., Díaz, S., Lavorel, S., Prentice, I.C., Leadley, P., Tautenhahn, S., Werner, G.D.A., Aakala, T., Abedi, M., Acosta, A.T.R., Adamidis, G.C., Adamson, K., Aiba, M., Albert, C.H., Alcántara, J.M., Alcázar C, C., Aleixo, I., Ali, H., Amiaud, B., Ammer, C., Amoroso, M.M., Anand, M., Anderson, C., Anten, N., Antos, J., Apgaua, D.M.G., Ashman, T.-L., Asmara, D.H., Asner, G.P., Aspinwall, M., Atkin, O., Aubin, I., Baastrup-Spohr, L., Bahalkeh, K., Bahn, M., Baker, T., Baker, W.J., Bakker, J.P., Baldocchi, D., Baltzer, J., Banerjee, A., Baranger, A., Barlow, J., Barneche, D.R., Baruch, Z., Bastianelli, D., Battles, J., Bauerle, W., Bauters, M., Bazzato, E., Beckmann, M., Beeckman, H., Beierkuhnlein, C., Bekker, R., Belfry, G., Belluau, M., Beloiu, M., Benavides, R., Benomar, L., Berdugo-Lattke, M.L., Berenguer, E., Bergamin, R., Bergmann, J., Bergmann Carlucci, M., Berner, L., Bernhardt-Römermann, M., Bigler, C., Bjorkman, A.D., Blackman, C., Blanco, C., Blonder, B., Blumenthal, D., Bocanegra-González, K.T., Boeckx, P., Bohlman, S., Böhning-Gaese, K., Boisvert-Marsh, L., Bond, W., Bond-Lamberty, B., Boom, A., Boonman, C.C.F., Bordin, K., Boughton, E.H., Boukili, V., Bowman, D.M.J.S., Bravo, S., Brendel, M.R., Broadley, M.R., Brown, K.A., Bruelheide, H., Brumnich, F., Bruun, H.H., Bruy, D., Buchanan, S.W., Bucher, S.F., Buchmann, N., Buitenwerf, R., Bunker, D.E., Bürger, J., Burrascano, S., Burslem, D.F.R.P., Butterfield, B.J., Byun, C., Marques, M., Scalon, M.C., Caccianiga, M., Cadotte, M., Cailleret, M., Camac, J., Camarero, J.J., Campany, C., Campetella, G., Campos, J.A., Cano-Arboleda, L., Canullo, R., Carbognani, M., Carvalho, F., Casanoves, F., Castagneyrol, B., Catford, J. A., Cavender-Bares, J., Cerabolini, B.E.L., Cervellini, M., Chacón-Madrigal, E., Chapin, K., Chapin, F.S., Chelli, S., Chen, S.-C., Chen, A., Cherubini, P., Chianucci, F., Choat, B., Chung, K.-S., Chytrý, M., Ciccarelli, D., Coll, L., Collins, C.G., Conti, L., Coomes, D., Cornelissen, J.H.C., Cornwell, W.K., Corona, P., Coyea, M., Craine, J., Craven, D., Cromsigt, J.P.G.M., Csecserits, A., Cufar, K., Cuntz, M., da Silva, A.C., Dahlin, K.M., Dainese, M., Dalke, I., Dalle Fratte, M., Dang-Le, A.T., Danihelka, J., Dannoura, M., Dawson, S., de Beer, A.J., De Frutos, A., De Long, J.R., Dechant, B., Delagrange, S., Delpierre, N., Derroire, G., Dias, A.S., Diaz-Toribio, M.H., Dimitrakopoulos, P.G., Dobrowolski, M., Doktor, D., Dřevojan, P., Dong, N., Dransfield, J., Dressler, S., Duarte, L., Ducouret, E., Dullinger, S., Durka, W., Duursma, R., Dymova, O., E-Vojtkó, A., Eckstein, R.L., Ejtehadi, H., Elser, J., Emilio, T., Engemann, K., Erfanian, M.B., Erfmeier, A., Esquivel-Muelbert, A., Esser, G., Estiarte, M., Domingues, T.F., Fagan, W.F., Fagúndez, J., Falster, D.S., Fan, Y., Fang, J., Farris, E., Fazlioglu, F., Feng, Y., Fernandez-Mendez, F., Ferrara, C., Ferreira, J., Fidelis, A., Finegan, B., Firn, J., Flowers, T.J., Flynn, D.F.B., Fontana, V., Forey, E., Forgiarini, C., François, L., Frangipani, M., Frank, D., Frenette-Dussault, C., Freschet, G.T., Fry, E.L., Fyllas, N.M., Mazzochini, G.G., Gachet, S., Gallagher, R., Ganade, G., Ganga, F., García-Palacios, P., Gargaglione, V., Garnier, E., Garrido, J.L., de Gasper, A.L., Gea-Izquierdo, G., Gibson, D., Gillison, A. N., Giroldo, A., Glasenhardt, M.-C., Gleason, S., Gliesch, M., Goldberg, E., Göldel, B., Gonzalez-Akre, E., Gonzalez-Andujar, J.L., González-Melo, A., González-Robles, A., Graae, B.J., Granda, E., Graves, S., Green, W.A., Gregor, T., Gross, N., Guerin, G.R., Günther, A., Gutiérrez, A.G., Haddock, L., Haines, A., Hall, J., Hambuckers, A., Han, W., Harrison, S.P., Hattingh, W., Hawes, J.E., He, T., He, P., Heberling, J.M., Helm, A., Hempel, S., Hentschel, J., Hérault, B., Hereş, A.-M., Herz, K., Heuertz, M., Hickler, T., Hietz, P., Higuchi, P., Hipp, A.L., Hirons, A., Hock, M., Hogan, J.A., Holl, K., Honnay, O., Hornstein, D., Hou, E., Hough-Snee, N., Hovstad, K.A., Ichie, T., Igić, B., Illa, E., Isaac, M., Ishihara, M., Ivanov, L., Ivanova, L., Iversen, C.M., Izquierdo, J., Jackson, R.B., Jackson, B., Jactel, H., Jagodzinski, A.M., Jandt, U., Jansen, S., Jenkins, T., Jentsch, A., Jespersen, J.R.P., Jiang, G.-F., Johansen, J.L., Johnson, D., Jokela, E.J., Joly, C.A., Jordan, G.J., Joseph, G.S., Junaedi, D., Junker, R.R., Justes, E., Kabzems, R., Kane, J., Kaplan, Z., Kattenborn, T., Kavelenova, L., Kearsley, E., Kempel, A., Kenzo, T., Kerkhoff, A., Khalil, M.I., Kinlock, N.L., Kissling, W.D., Kitajima, K., Kitzberger, T., Kjøller, R., Klein, T., Kleyer, M., Klimešová, J., Klipel, J., Kloeppel, B., Klotz, S., Knops, J.M.H., Kohyama, T., Koike, F., Kollmann, J., Komac, B., Komatsu, K., König, C., Kraft, N.J. B., Kramer, K., Kreft, H., Kühn, I., Kumarathunge, D., Kuppler, J., Kurokawa, H., Kurosawa, Y., Kuyah, S., Laclau, J.-P., Lafleur, B., Lallai, E., Lamb, E., Lamprecht, A., Larkin, D.J., Laughlin, D., Le Bagousse-Pinguet, Y., le Maire, G., le Roux, P.C., le Roux, E., Lee, T., Lens, F., Lewis, S.L., Lhotsky, B., Li, Y., Li, X., Lichstein, J.W., Liebergesell, M., Lim, J.Y., Lin, Y.-S., Linares, J.C., Liu, C., Liu, D., Liu, U., Livingstone, S., Llusià, J., Lohbeck, M., López-García, Á., Lopez-Gonzalez, G., Lososová, Z., Louault, F., Lukács, B.A., Lukeš, P., Luo, Y., Lussu, M., Ma, S., Maciel Rabelo Pereira, C., Mack, M., Maire, V., Mäkelä, A., Mäkinen, H., Malhado, A.C.M., Mallik, A., Manning, P., Manzoni, S., Marchetti, Z., Marchino, L., Marcilio-Silva, V., Marcon, E., Marignani, M., Markesteijn, L., Martin, A., Martínez-Garza, C., Martínez-Vilalta, J., Mašková, T., Mason, K., Mason, N., Massad, T.J., Masse, J., Mayrose, I., McCarthy, J., McCormack, M.L., McCulloh, K., McFadden, I.R., McGill, B.J., McPartland, M.Y., Medeiros, J.S., Medlyn, B., Meerts, P., Mehrabi, Z., Meir, P., Melo, F.P.L., Mencuccini, M., Meredieu, C., Messier, J., Mészáros, I., Metsaranta, J., Michaletz, S.T., Michelaki, C., Migalina, S., Milla, R., Miller, J.E.D., Minden, V., Ming, R., Mokany, K., Moles, A.T., Molnár, A., Molofsky, J., Molz, M., Montgomery, R.A., Monty, A., Moravcová, L., Moreno-Martínez, A., Moretti, M., Mori, A.S., Mori, S., Morris, D., Morrison, J., Mucina, L., Mueller, S., Muir, C.D., Müller, S.C., Munoz, F., Myers-Smith, I.H., Myster, R.W., Nagano, M., Naidu, S., Narayanan, A., Natesan, B., Negoita, L., Nelson, A.S., Neuschulz, E.L., Ni, J., Niedrist, G., Nieto, J., Niinemets, Ü., Nolan, R., Nottebrock, H., Nouvellon, Y., Novakovskiy, A., Nystuen, K.O., O'Grady, A., O'Hara, K., O'Reilly-Nugent, A., Oakley, S., Oberhuber, W., Ohtsuka, T., Oliveira, R., Öllerer, K., Olson, M.E., Onipchenko, V., Onoda, Y., Onstein, R.E., Ordonez, J.C., Osada, N., Ostonen, I., Ottaviani, G., Otto, S., Overbeck, G.E., Ozinga, W.A., Pahl, A.T., Paine, C.E.T., Pakeman, R.J., Papageorgiou, A.C., Parfionova, E., Pärtel, M., Patacca, M., Paula, S., Paule, J., Pauli, H., Pausas, J.G., Peco, B., Penuelas, J., Perea, A., Peri, P.L., Petisco-Souza, A.C., Petraglia, A., Petritan, A.M., Phillips, O.L., Pierce, S., Pillar, V.D., Pisek, J., Pomogaybin, A., Poorter, H., Portsmuth, A., Poschlod, P., Potvin, C., Pounds, D., Powell, A.S., Power, S.A., Prinzing, A., Puglielli, G., Pyšek, P., Raevel, V., Rammig, A., Ransijn, J., Ray, C.A., Reich, P.B., Reichstein, M., Reid, D.E.B., Réjou-

Méchain, M., de Dios, V.R., Ribeiro, S., Richardson, S., Riibak, K., Rillig, M.C., Riviera, F., Robert, E.M.R., Roberts, S., Robroek, B., Roddy, A., Rodrigues, A.V., Rogers, A., Rollinson, E., Rolo, V., Römermann, C., Ronzhina, D., Roscher, C., Rosell, J.A., Rosenfield, M.F., Rossi, C., Roy, D.B., Royer-Tardif, S., Rüger, N., Ruiz-Peinado, R., Rumpf, S.B., Rusch, G.M., Ryo, M., Sack, L., Saldaña, A., Salgado-Negret, B., Salguero-Gomez, R., Santa-Regina, I., Santacruz-García, A.C., Santos, J., Sardans, J., Schamp, B., Scherer-Lorenzen, M., Schleuning, M., Schmid, B., Schmidt, M., Schmitt, S., Schneider, J.V., Schowanek, S.D., Schrader, J., Schrodt, F., Schuldt, B., Schurr, F., Selaya Garvizu, G., Semchenko, M., Seymour, C., Sfair, J.C., Sharpe, J.M., Sheppard, C.S., Sheremetiev, S., Shiodera, S., Shipley, B., Shovon, T.A., Siebenkäs, A., Sierra, C., Silva, V., Silva, M., Sitzia, T., Sjöman, H., Slot, M., Smith, N. G., Sodhi, D., Soltis, P., Soltis, D., Somers, B., Sonnier, G., Sørensen, M.V., Sosinski, E. E., Soudzilovskaia, N.A., Souza, A.F., Spasojevic, M., Sperandii, M.G., Stan, A.B., Stegen, J., Steinbauer, K., Stephan, J.G., Sterck, F., Stojanovic, D.B., Strydom, T., Suarez, M.L., Svenning, J.-C., Svitková, I., Svitok, M., Svoboda, M., Swaine, E., Swenson, N., Tabarelli, M., Takagi, K., Tappeiner, U., Tarifa, R., Tauugourdeau, S., Tavsanoglu, C., te Beest, M., Tedersoo, L., Thiffault, N., Thom, D., Thomas, E., Thompson, K., Thornton, P.E., Thuiller, W., Tichý, L., Tissue, D., Tjoelker, M.G., Tng, D.Y.P., Tobias, J., Török, P., Tarin, T., Torres-Ruiz, J.M., Tóthmérész, B., Treurnicht, M., Trivellone, V., Trolliet, F., Trotsiuk, V., Tsakalos, J.L., Tsiripidis, I., Tysklind, N., Umehara, T., Usoltsev, V., Vadeboncoeur, M., Vaezi, J., Valladares, F., Vamosi, J., van Bodegom, P.M., van Breugel, M., Van Cleemput, E., van de Weg, M., van der Merwe, S., van der Plas, F., van der Sande, M.T., van Kleunen, M., Van Meerbeek, K., Vanderwel, M., Vanselow, K.A., Vårhammar, A., Varone, L., Vasquez Valderrama, M.Y., Vassilev, K., Vellend, M., Veneklaas, E.J., Verbeeck, H., Verheyen, K., Vibrans, A., Vieira, I., Villacís, J., Violle, C., Vivek, P., Wagner, K., Waldram, M., Waldron, A., Walker, A.P., Waller, M., Walther, G., Wang, H., Wang, F., Wang, W., Watkins, H., Watkins, J., Weber, U., Weedon, J.T., Wei, L., Weigelt, P., Weiher, E., Wells, A.W., Wellstein, C., Wenk, E., Westoby, M., Westwood, A., White, P.J., Whitten, M., Williams, M., Winkler, D.E., Winter, K., Womack, C., Wright, I.J., Wright, S.J., Wright, J., Pinho, B.X., Ximenes, F., Yamada, T., Yamaji, K., Yanai, R., Yankov, N., Yguel, B., Zanini, K.J., Zanne, A.E., Zelený, D., Zhao, Y.-P., Zheng, J., Zheng, J.i., Ziemińska, K., Zirbel, C.R., Zizka, G., Zo-Bi, I.C., Zotz, G., Wirth, C., 2020. TRY plant trait database – enhanced coverage and open access. Glob. Chang. Biol. 26 (1), 119–188.

Kirwan, M.L., Gedan, K.B., 2019. Sea-level driven land conversion and the formation of ghost forests. Nat. Clim. Chang. 9 (6), 450–457.

Kozlowski, T.T., Pallardy, S.G., 1997. The Physiological Ecology of Woody Plants. Academic Press, San Diego, p. 410.

Larsen, A.E., Meng, K., Kendall, B.E., O'Hara, R.B., 2019. Causal analysis in control–impact ecological studies with observational data. Methods Ecol. Evol. 10 (7), 924–934.

Le Dantec, V., Dufrêne, E., Saugier, B., 2000. Interannual and spatial variation in maximum leaf area index of temperate deciduous stands. For. Ecol. Manage. 134 (1-3), 71–81.

LeBauer, D.S., Wang, D., Richter, K.T., Davidson, C.C., Dietze, M.C., 2013. Facilitating feedbacks between field measurements and ecosystem models. Ecol. Monogr. 83 (2), 133–154.

Liu, F., Yang, W., Wang, Z., Xu, Z., Liu, H., Zhang, M., Liu, Y., An, S., Sun, S., 2010. Plant size effects on the relationships among specific leaf area, leaf nutrient content, and photosynthetic capacity in tropical woody species. Acta Oecol. 36 (2), 149–159.

Liu, Z., Zhao, M., Zhang, H., Ren, T., Liu, C., He, N., 2023. Divergent response and adaptation of specific leaf area to environmental change at different spatio-temporal scales jointly improve plant survival. Glob. Chang. Biol. 29 (4), 1144–1159.

Maire, V., Wright, I.J., Prentice, I.C., Batjes, N.H., Bhaskar, R., van Bodegom, P.M., Cornwell, W.K., Ellsworth, D., Niinemets, Ü., Ordonez, A., Reich, P.B., Santiago, L.S., 2015. Global effects of soil and climate on leaf photosynthetic traits and rates. Glob. Ecol. Biogeogr. 24 (6), 706–717.

Marshall, J.D., Monserud, R.A., 2003. Foliage height influences specific leaf area of three conifer species. Can. J. For. Res. 33 (1), 164–170.

McDowell, N.G., Ball, M., Bond-Lamberty, B., Kirwan, M.L., Krauss, K.W., Megonigal, J. P., Mencuccini, M., Ward, N.D., Weintraub, M.N., Bailey, V., 2022. Processes and mechanisms of coastal woody-plant mortality. Glob. Chang. Biol. 28 (20), 5881–5900.

Mollick, A.S., Sultana, R., Azad, M.S., Khan, M.N.I., 2021. Leaf morphological plasticity in three dominant tree species in the Sundarbans mangrove forest of Bangladesh in different salinity zones. Wetl. Ecol. Manag. 29 (2), 265–279.

Munns, R., 2002. Comparative physiology of salt and water stress. Plant Cell Environ. 25, 239–250.

Mussche, S., Samson, R., Nachtergale, L., De Schrijver, A., Lemeur, R., Lust, N., 2001. A comparison of optical and direct methods for monitoring the seasonal dynamics of leaf area index in deciduous forests. Silva Fenn. 35. https://doi.org/10.14214/sf.575,.

Negrão, S., Schmöckel, S.M., Tester, M., 2017. Evaluating physiological responses of plants to salinity stress. Ann. Bot. 119 (1), 1–11.

Niinemets, Ü., Tenhunen, J.D., Canta, N.R., Chaves, M.M., Faria, T., Pereira, J.S., Reynolds, J.F., 1999. Interactive effects of nitrogen and phosphorus on the acclimation potential of foliage photosynthetic properties of cork oak, Quercus suber, to elevated atmospheric CO_2concentrations. Glob. Chang. Biol. 5 (4), 455–470.

National Ecological Observatory Network: Data Product DP1.10033.001, Litterfall and fine woody debris production and chemistry (provisional data). Battelle, Boulder, CO, USA NEON. 2021, 2021.

Park, H., Jeong, S., 2021. Leaf area index in Earth system models: how the key variable of vegetation seasonality works in climate projections. Environ. Res. Lett. 16 (3), 034027.

Parker, G. G. and Tibbs, D. J.: Structural Phenology of the Leaf Community in the Canopy of a Liriodendron tulipifera L. Forest in Maryland, USA, For. Sci., 50, 387, 2004.

Parker, G.G., O'Neill, J.P., Higman, D., 1989. Vertical profile and canopy organization in a mixed deciduous forest. Vegetatio 85 (1-2), 1–11.

Pennington, S.C., McDowell, N.G., Megonigal, J.P., Stegen, J.C., Bond-Lamberty, B., 2020. Localized basal area affects soil respiration temperature sensitivity in a coastal deciduous forest. Biogeosciences 17, 771–780.

Pezeshki, S.R., Delaune, R.D., Patrick, W.H., 1990. Flooding and saltwater intrusion: Potential effects on survival and productivity of wetland forests along the U.S. Gulf Coast. For. Ecol. Manage. 33-34, 287–301.

Pitz, S., Megonigal, J.P., 2017. Temperate forest methane sink diminished by tree emissions. New Phytol. 214 (4), 1432–1439.

R Core Team: R: A Language and Environment for Statistical Computing v4.1.0, R Foundation for Statistical Computing, Vienna, Austria, 2021.

Reich, P.B., Wright, I.J., Lusk, C.H., 2007. Predicting leaf physiology from simple plant and climate attributes: A global GLOPNET analysis. Ecol. Appl. 17 (7), 1982–1988.

Rodríguez, P., Torrecillas, A., Morales, M. A., Ortuño, M. F., and Sánchez-Blanco, M. J.: Effects of NaCl salinity and water stress on growth and leaf water relations of Asteriscus maritimus plants, Environ. Exp. Bot., 53, 113–123, 2005.

Schimel, D., Hargrove, W., Hoffman, F., MacMahon, J., 2007. NEON: a hierarchically designed national ecological network. Front. Ecol. Environ. 5 (2), 59.

Sellin, A., Kupper, P., 2006. Spatial variation in sapwood area to leaf area ratio and specific leaf area within a crown of silver birch. Trees 20 (3), 311–319.

Shiklomanov, A.N., Bond-Lamberty, B., Atkins, J.W., Gough, C.M., 2020. Structure and parameter uncertainty in centennial projections of forest community structure and carbon cycling. Glob. Chang. Biol. 26 (11), 6080–6096.

Sinha, E., Calvin, K.V., Bond-Lamberty, B., Drewniak, B.A., Ricciuto, D.M., Sargsyan, K., Cheng, Y., Bernacchi, C., Moore, C.E., 2023. Modeling perennial bioenergy crops in the E3SM land model (ELMv2). J. Adv. Model. Earth Syst. 15 (1) https://doi.org/10.1029/2022ms003171.

Ury, E.A., Yang, X.i., Wright, J.P., Bernhardt, E.S., 2021. P.: Rapid deforestation of a coastal landscape driven by sea-level rise and extreme events. Ecological 31 (5).

Venables, W.N., Ripley, B., 2003. D.: Modern Applied Statistics in S, Fourth edition.,. Springer-Verlag, New York, p. 512 pp.,.

Vovides, A.G., Vogt, J., Kollert, A., Berger, U., Grueters, U., Peters, R., Lara-Domínguez, A.L., López-Portillo, J., 2014. Morphological plasticity in mangrove trees: salinity-related changes in the allometry of Avicennia germinans. Trees 28 (5), 1413–1425.

Walker, A.P., Hanson, P.J., De Kauwe, M.G., Medlyn, B.E., Zaehle, S., Asao, S., Dietze, M., Hickler, T., Huntingford, C., Iversen, C.M., Jain, A., Lomas, M., Luo, Y., McCarthy, H., Parton, W.J., Prentice, I.C., Thornton, P.E., Wang, S., Wang, Y.-P., Warlind, D., Weng, E., Warren, J.M., Woodward, F.I., Oren, R., Norby, R.J., 2014. Comprehensive ecosystem model-data synthesis using multiple data sets at two temperate forest free-air CO2 enrichment experiments: Model performance at ambient CO2 concentration. Journal of Geophysical Research-Biogeosciences 119 (5), 937–964.

Wang, W., McDowell, N.G., Pennington, S., Grossiord, C., Leff, R.T., Sengupta, A., Ward, N.D., Sezen, U.U., Rich, R., Megonigal, J.P., Stegen, J.C., Bond-Lamberty, B., Bailey, V., 2020. Tree growth, transpiration, and water-use efficiency between shoreline and upland red maple (Acer rubrum) trees in a coastal forest. Agric. For. Meteorol. 295, 108163.

Wang, H., Prentice, I.C., Wright, I.J., Warton, D.I., Qiao, S., Xu, X., Zhou, J., Kikuzawa, K., Stenseth, N., 2023. C.: Leaf economics fundamentals explained by optimality principles. Sci. Adv. 9, eadd5667.

Ward, N.D., Megonigal, J.P., Bond-Lamberty, B., Bailey, V.L., Butman, D., Canuel, E.A., Diefenderfer, H., Ganju, N.K., Goñi, M.A., Graham, E.B., Hopkinson, C.S., Khangaonkar, T., Langley, J.A., McDowell, N.G., Myers-Pigg, A.N., Neumann, R.B., Osburn, C.L., Price, R.M., Rowland, J., Sengupta, A., Simard, M., Thornton, P.E., Tzortziou, M., Vargas, R., Weisenhorn, P.B., Windham-Myers, L., 2020. Representing the function and sensitivity of coastal interfaces in Earth system models. Nat. Commun. 11, 2458.

Williams, S.J., 2013. Sea-level rise implications for coastal regions. J. Coast. Res. 63, 184–196.

Woods, N.N., Swall, J.L., Zinnert, J.C., 2020. Soil Salinity Impacts Future Community Composition of Coastal Forests. Wetlands 40 (5), 1495–1503.

Wright, I.J., Reich, P.B., Westoby, M., Ackerly, D.D., Baruch, Z., Bongers, F., Cavender-Bares, J., Chapin, T., Cornelissen, J.H.C., Diemer, M., Flexas, J., Garnier, E., Groom, P.K., Gulias, J., Hikosaka, K., Lamont, B.B., Lee, T., Lee, W., Lusk, C., Midgley, J.J., Navas, M.-L., Niinemets, Ü., Oleksyn, J., Osada, N., Poorter, H., Poot, P., Prior, L., Pyankov, V.I., Roumet, C., Thomas, S.C., Tjoelker, M.G., Veneklaas, E.J., Villar, R., 2004. The worldwide leaf economics spectrum. Nature 428 (6985), 821–827.

Xiao, C.-W., Janssens, I.A., Curiel Yuste, J., Ceulemans, R., 2006. Variation of specific leaf area and upscaling to leaf area index in mature Scots pine. Trees 20 (3), 304–310.

Yang, X.u., Szlavecz, K., Pitz, S.L., Langley, J.A., Chang, C.-H., 2020. The partitioning of litter carbon fates during decomposition under different rainfall patterns: a laboratory study. Biogeochemistry 148 (2), 153–168.

Zhai, L., Krauss, K.W., Liu, X., Duberstein, J.A., Conner, W.H., DeAngelis, D.L., Sternberg, L., 2018. Growth stress response to sea level rise in species with contrasting functional traits: A case study in tidal freshwater forested wetlands. Environ. Exp. Bot. 155, 378–386.

Zheng, G., Moskal, L.M., 2012. Spatial variability of terrestrial laser scanning based leaf area index. Int. J. Appl. Earth Obs. Geoinf. 19, 226–237.